AAPS PharmSciTech, Vol. 17, No. 5, October 2016 (© 2015)
DOI: 10.1208/s12249-015-0460-4

Research Article

In Vitro Release and Bioavailability of Silybin from Micelle-Templated Porous Calcium Phosphate Microparticles

Yuan Zhu,[1] Miaomiao Wang,[1] Ya Zhang,[1] Jin Zeng,[1] E. Omari-Siaw,[1] Jiangnan Yu,[1] and Ximing Xu[1,2,3]

Received 3 August 2015; accepted 30 November 2015; published online 15 December 2015

ABSTRACT. Developing a promising carrier for the delivery of poorly water-soluble drugs, such as silybin, to improve oral absorption has become a very worthy of consideration. The goal of this study was to prepare a novel porous calcium phosphate microparticle using povidone-mixed micelles as template while evaluating its *in vitro* and *in vivo* properties with silybin as a model drug. The particle characterization, *in vitro* drug release behavior, and pharmacokinetic parameters of the prepared silybin-loaded calcium phosphate microparticle were investigated. The mean particle size was found to be 3.54±0.32 μm with a rough surface porous structure. Additionally, the silybin-loaded calcium phosphate microparticle compared with the free silybin showed a prolonged 72-h release *in vitro* and a higher C_{max} (418.5± 23.7 ng mL^{-1}) with 167.5% oral relative bioavailability. A level A *in vitro–in vivo* correlation (IVIVC), established for the first time, demonstrated an excellent IVIVC of the formulated silybin in oral administration. In conclusion, this povidone-mixed micelle-based microparticle was successfully prepared to enhance the oral bioavailability of silybin. Therefore, application of this novel porous calcium phosphate microparticle holds a significant potential for the development of poorly water-soluble drugs.

KEY WORDS: bioavailability; calcium phosphate; porous microparticles; povidone-mixed micelle; silybin.

INTRODUCTION

Calcium phosphate has been extensively researched as the biocompatible inorganic biomaterial for synthetic bone grafts (1) and non-viral vectors for gene delivery (2). Over the past decades, the application of porous calcium phosphate as carriers in drug delivery has attracted much attention due to significant advantages such as large specific surface area and high loading capacity for drug (3), protein (4,5), or DNA molecules (6,7). Among the application methods which include micelle-templated synthesis (8,9), emulsion process (10–12), and surfactant-assisted route (13,14), micelle-templated synthesis technique has been the most widely used. To date, polymeric micelle templates have been successfully applied to the fabrication of many porous calcium phosphate carriers. One salient feature of such carriers prepared with micelle-templated method is the ease to tune size and morphology by adjusting the polymer combination, mineralization time, and solvent composition. Afterwards, the micelle template can be removed by calcination or solvent evaporation, leading to a porous or hollow structure.

The key to a successful micelle-templated synthesis is to prepare a proper micelle as template. Our previous work on the polyvinylpyrrolidone (PVP)/sodium cholate/phospholipid mixed (povidone-mixed) micelle (15,16) established it as a novel carrier which was good at improving the solubility and oral bioavailability of poorly water-soluble drugs. Also, the auxiliary material PVP, a water-soluble nonionic polymer, has a long history in pharmaceutical application as a delivery system for hydrophobic drugs (17). Besides, the bile salts have been shown to enhance the solubility of hydrophobic drugs (18,19). Hence, with the aid of such a micelle system, a controlled architecture of calcium phosphate with porous or hollow structure could be designed to facilitate drug delivery. Thus, the present study aimed at obtaining a porous calcium phosphate carrier for hydrophobic drugs by a new type of polymeric micelle and focused on developing a promising oral carrier for potential applications to improve the delivery of poorly water-soluble drugs *in vitro* and *in vivo*.

Despite increasing interests of calcium phosphate carriers in drug delivery (20,21), very limited numbers of studies regarding its oral administration exist. Therefore, to evaluate its drug release and oral administration efficiencies, silybin, a naturally occurring polyphenolic flavonoid extracted from the seed of the milk thistle (*Silybum marianum*) (22,23), was incorporated into the calcium phosphate micron-sized carrier as a model drug in this work. Silybin has been widely used for the treatment of liver disorders (24,25), such as chronic active

Yuan Zhu and Miaomiao Wang contributed equally to this work.

[1] Department of Pharmaceutics, School of Pharmacy, Center for Nano Drug/Gene Delivery and Tissue Engineering, Jiangsu University, Zhenjiang, 212001, People's Republic of China.
[2] Department of Pharmaceutics, School of Pharmacy, Center for Nano Drug/Gene Delivery and Tissue Engineering, Jiangsu University, Zhenjiang, 212013, People's Republic of China.
[3] To whom correspondence should be addressed. (e-mail: xmxu@ujs.edu.cn)

hepatitis, hepatic cirrhosis, as well as alcohol-, drug-, and toxin-induced liver damage (26,27).

Herein, attempts at preparing a novel calcium phosphate micron-sized carrier based on povidone-mixed micelle (16) to improve *in vitro* release and oral bioavailability of the poorly water-soluble drug, silybin, have been carried out in this work.

MATERIALS AND METHODS

Materials

Phospholipid was purchased from Taiwei Pharmaceutical Industry Co., Ltd (Shanghai, China). Sodium cholate, disodium hydrogen phosphate, and calcium chloride were obtained from Sinopharm Chemical Reagent Co., Ltd (Shanghai, China). PVP K30 of pharmaceutical grade (Mw ~ 45,000) was purchased from Sunpower New Material Co., Ltd (Shanghai, China). Silybin (purity ≥ 98%) was kindly provided by Zhongxing Pharmaceutical Industry Co., Ltd (Jiangsu, China). α-Naphthol was purchased from Tianjin Chemical Reagent Factory (Tianjin, China). Other chemical reagents were of analytical grade or better. Male beagle dogs (2 years old, weighing 10.1 ± 1.9 kg) were purchased from Yadong Laboratory Animal Research Center (Jiangsu, China). All the experimental protocols involving animals in this study were evaluated and approved by the Ethics Committee of Jiangsu University on March 2, 2013. The number of the certification which verified approval of this study is 20130302-1.

Preparation of Calcium Phosphate Microparticles

Calcium phosphate microparticles were prepared according to our previous studies (28). In brief, absolute ethanol solution (20 mL) containing sodium cholate (0.7 g) and phospholipid (0.3 g) was added to 50 mM $CaCl_2$ aqueous solution (60 mL) and stirred vigorously at 40°C for 10 min. Na_2HPO_4 (50 mM, 40 mL) and absolute ethanol solution (20 mL) containing PVP K30 (0.4 g) were added drop-wise to the mixture. The suspension obtained was then stirred at 600 rpm for 12 h. The resulting white precipitate was collected and washed thrice by centrifugation-redispersion cycles with deionized water and absolute ethanol. Finally, the collected precipitates were freeze-dried to obtain the powder of calcium phosphate microparticles.

Preparation of Silybin-Loaded Calcium Phosphate Microparticles

The calcium phosphate microparticles were suspended in deionized water to obtain a concentration of 50 mg mL^{-1}. Then, a 100-mg mL^{-1} silybin solution was prepared using absolute ethanol as solvent. The calcium phosphate microparticles and silybin solution were mixed at the proportion of 2:1 (*v*/*v*) at 37°C and stirred at 600 rpm for 12 h. After centrifugation for 10 min at 15,000 rpm and washing three times with absolute ethanol, the silybin-loaded calcium phosphate microparticles were collected. The powders of silybin-loaded calcium phosphate microparticles were obtained by a freeze-drying process and kept at 4°C for further evaluation.

Particle Size Analysis

Dynamic light scattering measurement was carried out to determine the particle size distribution of calcium phosphate microparticle suspension in deionized water (3 mL, 10 mg mL^{-1}) using BIC90 Nanoparticle Size Analyzer (Brookhaven Instruments, USA) at 25°C. The mean particle size was analyzed by the dispersion technology software (Brookhaven Instruments, USA). All assays were performed in triplicate.

Scanning Electron Microscopy (SEM)

The powders of calcium phosphate microparticles were platinum coated with thickness in the range of 3–5 nm. The SEM images of calcium phosphate microparticles were recorded using a JSM 7001F scanning electron microscope (JEOL, Japan) at a working distance of 8 mm and an acceleration voltage of 15 kV.

Fourier Transform Infrared Spectroscopy (FTIR)

To confirm the successful incorporation of silybin, the FTIR spectral measurements were performed using a Nicolet spectrophotometer (Model Avatar 370, Milwaukee, WI, USA). The samples were finely ground with KBr to prepare the pellets under a hydraulic pressure of 8 mPa, and the spectra were scanned between 400 and 4000 cm^{-1}.

Drug Loading

The silybin-loaded calcium phosphate microparticles were washed thrice with absolute ethanol to dissolve the unloaded silybin. The volume of the eluent was determined and, after diluting to a suitable concentration, the resulting ethanol solution was analyzed by UV at 288 nm, according to the previous literature (29). The absorbance recorded was applied to a standard curve formula to calculate the concentration of silybin in the ethanol solution. The standard curve formula ($A = 0.042236C - 0.0043510$ ($n = 6$, $r = 0.99939$) where A was the absorbance at 288 nm and C represented the concentration of silybin) was established by determining the absorbance of a series of standard silybin ethanol solutions (1, 5, 10, 15, 20, and 30 μg mL^{-1}). The data of drug loading presented as mean of triplicate samples was calculated according to the following equation:

$$\text{Drug loading} = 100\%(W_1 - W_2)/W$$

where W was the total weight of drug-loaded calcium phosphate microparticles, W_1 was the weight of drug which was used to prepare the sample of silybin-loaded calcium phosphate microparticles, and W_2 was the weight of drug in the eluent.

In Vitro Drug Release

The *in vitro* release of silybin-loaded calcium phosphate microparticles and free silybin were investigated with a dialysis method in two different media, phosphate buffer solution

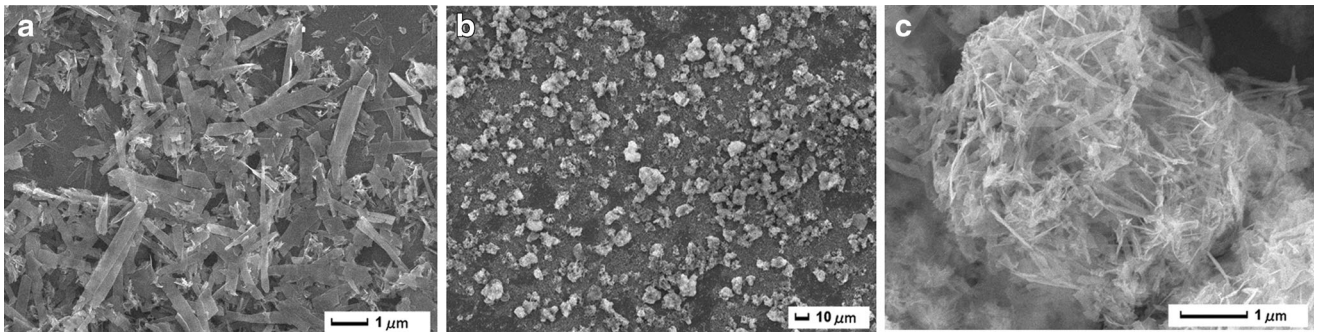

Fig. 1. Scanning electron micrograph of **a** calcium phosphate microparticles without micelle template, **b** porous calcium phosphate microparticles at ×1000 magnification, and **c** calcium phosphate microparticles at ×10,000 magnification

(pH 7.4) and HCl solution (pH 1.2), using a ZRS-8G dissolution test apparatus (Tianjin Tianda Tianfa, China). Sample powder (50 mg) was dispersed in 1 mL of each dissolution medium, before placing in dialysis bag (Mw ~ 3500). The dialysis bag was placed in the basket before immersing in 900 mL of media at 37±0.5°C with a rotational paddle speed of 100± 2 rpm. At settled time intervals (0.5, 1, 2, 3, 6, 8, 12, 24, 36, 48, 60, and 72 h), the dissolution medium of 5 mL was withdrawn and replaced with equal volume of fresh medium (preheated to 37°C). The samples at each time points were filtered through 0.45 μm cellulose nitrate membranes for UV analysis at 288 nm. The calibration tests made with UV absorption measurements of pure silybin at different pH values showed no change in the drug spectra. The cumulative release (%) was calculated as the weight ratio of released silybin to total silybin. Data at each time point were presented as mean of triplicate samples.

Bioavailability of Silybin-Loaded Calcium Phosphate Microparticles in Beagle Dogs

Four male beagle dogs were randomly and equally divided into two groups. The beagle dogs were housed individually and acclimatized in the laboratory for at least 1 week prior to testing. Each dog was fasted for 24 h with free access to water before the experiment. Capsules filled with silybin-loaded calcium phosphate microparticle (at a dose of 20 mg kg^{-1} silybin) and free silybin were orally administered to each group of dogs, respectively. The washout period between two consecutive treatments was 2 weeks. After oral administration, 2 mL of blood samples was collected from the jugular vein into a heparinized tube at each time point of 0.25, 0.5, 1, 2, 4, 6, 8, 10, 12, and 24 h. The plasma obtained after centrifugation (10 min, 3000 rpm) was stored immediately at −20°C until analysis. Silybin in 200 μL of dog plasma was extracted by the addition of 20 μL internal standard solution (α-naphthol, 10 μg mL^{-1} in methanol), 200 μL KH_2PO_4 (0.2 mol L^{-1}, pH 5), 20 μL methanol, and 5 mL diethyl ether. The mixture was vortex-mixed thoroughly for 5 min and then centrifuged for 10 min at 3000 rpm. The organic phase (4 mL) was quantitatively transferred and evaporated to dryness under a nitrogen flow at 37°C. The dried residue was re-suspended in 100 μL mobile phase. The re-suspended solution (20 μL) was injected into an HPLC system. A Symmetry C18 reserved phase analytical column (5 μm, 4.6 mm×150 mm, Waters, USA) set at 38°C was employed. The mobile phase was a mixture of methanol and 0.05 mol L^{-1} KH_2PO_4 (*v*/*v* 1:1, pH adjusted to 3.8 with phosphoric acid) at 1.0 mL min^{-1} flow rate. The UV detection wavelength was set at 288 nm. The calibration was linear over a range from 10 to 1000 ng mL^{-1} (R=0.0014297C−0.010905) with a correlation coefficient (r) 0.99851. The LOD of current assay based on S/N=3 was 3 ng mL^{-1} in plasma. The method recoveries were all above 80% at high, middle, and low concentrations, and the intra- and inter-day variation was below to 10.0%. Since silybin is an isomeric compound, two peaks with the retention time were detected (30). The sum of the area of the two peaks was calculated for analysis. The ratio of peak area of silybin over that of the internal standard was used for quantitative analysis. And the method was validated by adding various quantities of silybin to blank beagle dog plasma. These calibrations were subjected to the entire analytical procedure, so as to test the linearity, precision, and accuracy of the method. The peak concentration (C_{max}) and peak time (T_{max}) were derived directly from the experimental points. The relative bioavailability and other pharmacokinetic parameters were calculated using the program BAPP 2.3 (supplied by the Center of Drug Metabolism and Pharmacokinetics, China Pharmaceutical University) by non-compartmental analysis.

In Vitro–In Vivo Correlation

In this study, a plot of percent dissolved *in vitro vs.* percent absorbed *in vivo* input at various time points up to

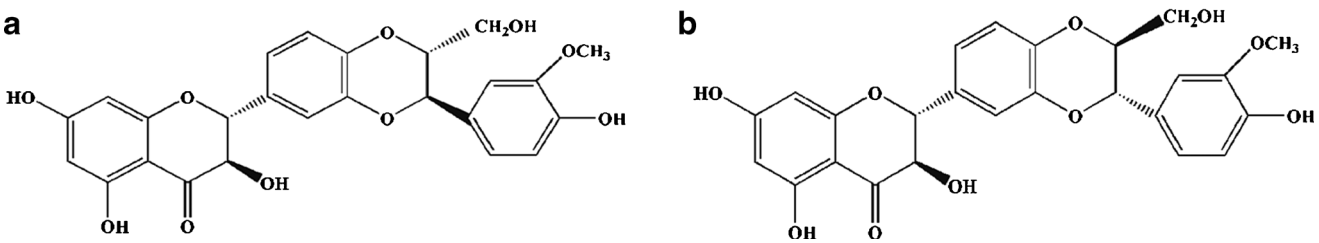

Fig. 2. Chemical structure of isomeric silybin: **a** silybin A, **b** silybin B

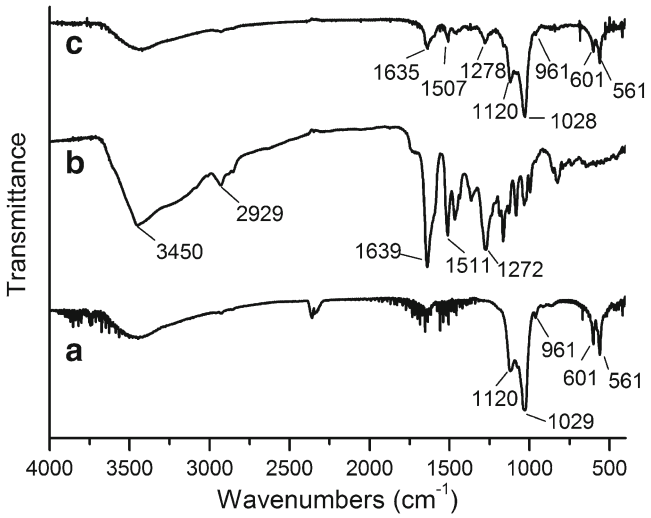

Fig. 3. FTIR spectra of **a** calcium phosphate microparticles, **b** silybin, and **c** silybin-loaded calcium phosphate microparticles

24 h was constructed to develop a level A correlation as classified by US Food and Drug Administration (31). Also, the correlation between *in vitro* release in two dissolution media (pH 7.4 phosphate buffer solution and pH 1.2 HCl solution) and the *in vivo* absorption was respectively established.

Statistical Analysis

All the experimental data were expressed as mean± standard deviation (SD), and the statistical differences between the different groups were evaluated by Student's *t* test. The SPSS statistic software (SPSS version 15.0, SPSS Inc., Chicago, IL, USA) was used. Difference between two groups was considered to be statistically significant at $p<0.05$.

RESULTS

Characterization of Calcium Phosphate Microparticles

Figure 1 illustrates SEM of the surface and integral morphology of the calcium phosphate microparticles. Significant differences were observed between Fig. 1a and b, which depicted the calcium phosphate microparticles without the micelle template and the porous calcium phosphate microparticles, respectively. Apparently, the calcium phosphate microparticles exhibited spherical or ellipsoidal shape with rough surfaces (Fig. 1b). A closer view of the micron-sized calcium phosphate carrier revealed a nest-like structure on the surface with particle size around 3.5 μm (Fig. 1c). This indicated an irregular porous structure resulting from the crystal assembling based on the

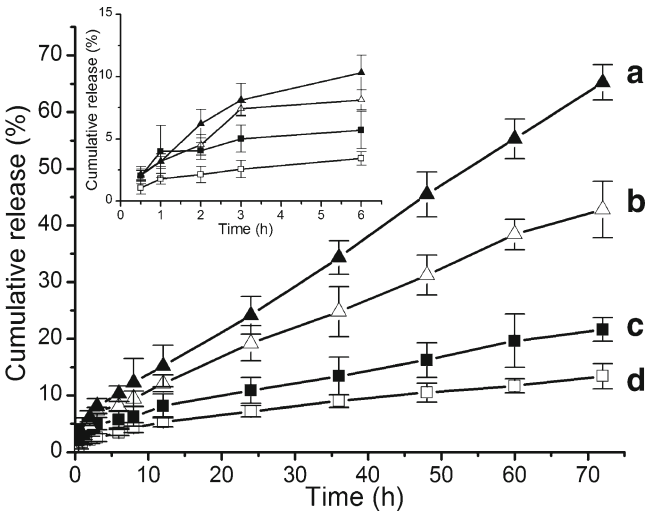

Fig. 4. *In vitro* release profiles of silybin-loaded calcium phosphate microparticles in **a** pH 7.4 phosphate buffer saline, **b** pH 1.2 HCl, and release profiles of free silybin in **c** pH 7.4 phosphate buffer saline and **d** pH 1.2 HCl (mean ± SD, $n=3$)

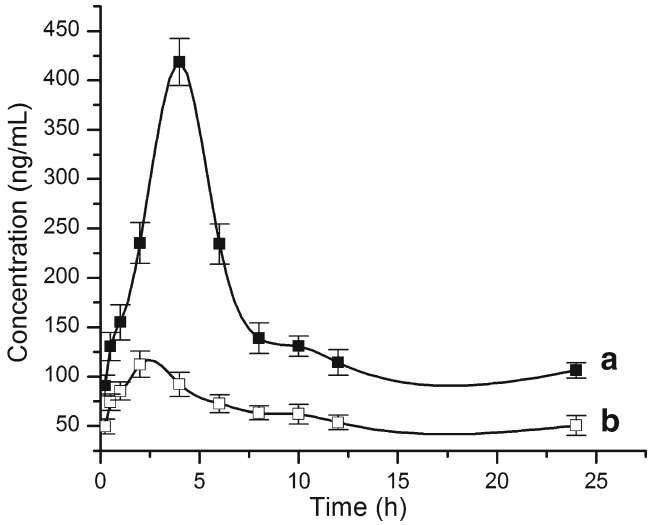

Fig. 5. Mean plasma concentration–time profiles of silybin in beagle dogs after oral administration of **a** silybin-loaded calcium phosphate microparticles and **b** free silybin equivalent to 20 mg kg^{-1} of silybin (mean ± SD, $n = 4$)

povidone-mixed micelle template. From the structure of silybin presented in Fig. 2 and the FTIR spectra shown in Fig. 3, characteristic phosphate group bands (Fig. 3a) occurred at wave numbers 561, 601, 961, 1029, and 1120 cm^{-1} for the calcium phosphate microparticles. The bands at 1029 and 1120 cm^{-1} could be assigned to the components of triply degenerate ν_3 antisymmetric P–O stretching mode. The non-degenerate P–O symmetric stretching mode ν_2 was detected at 961 cm^{-1}. The bands at 601 and 561 cm^{-1} could also be attributed to the components of the triply degenerated ν_1 O–P–O bending mode. The FTIR spectra in Fig. 3b indicated characteristic group bands at wave numbers 1272, 1511, 1639, 2929, and 3450 cm^{-1} for free silybin. The broader band at 3450 cm^{-1} was attributed to the hydroxyl groups, while the bands at 2929, 1639, 1272, and 1511 cm^{-1} were assigned to C–H, C=O, C–O, and C=C stretching modes, respectively, which proved the existence of benzene ring. The FTIR spectra in Fig. 3c showed both characteristic group bands of calcium phosphate and silybin. The bands at wave numbers 561, 601, 961, 1028, and 1120 cm^{-1} in the spectra indicated the presence of calcium phosphate. The characteristic groups of silybin could be assigned to the bands at wave numbers 1278, 1507, and 1635 cm^{-1}. The most noticeable change in the FTIR spectra shown in Fig. 3c was the disappearance of the O–H (3450 cm^{-1}) and C–H (2929 cm^{-1}) bands as well as the significant decrease of transmittance values at silybin characteristic group bands (1278, 1507, and 1635 cm^{-1}). These results suggest that silybin was loaded into the porous structure of calcium phosphate microparticles. The content of loaded silybin was calculated to be 44.6±1.2%.

In Vitro Drug Release

Figure 4 showed the dissolution profiles of silybin-loaded calcium phosphate microparticles and free silybin in HCl solution (pH 1.2) and phosphate buffer solution (pH 7.4).Less than 21.7% of the free silybin (suspended in 1 mL of the dissolution medium) in the dialysis bag was released within 72 h as compared to 65.2% from the calcium phosphate microparticles. The respective cumulative drug release of 13.4% and 42.8% from free silybin and the microparticle in HCl solution (pH 1.2) within 72 h was relatively slower as compared with that from the phosphate buffer saline (pH 7.4) over the same period. These results suggest that the release of silybin in this study was pH-dependent, with higher pH values leading to faster drug release.

Table I. The Main Pharmacokinetic Parameters of Silybin-Loaded Calcium Phosphate Microparticles and Free Silybin in Beagle Dogs ($n = 4$)

Parameters	Unit	Silybin-loaded calcium phosphate microparticles	Silybin
$t_{1/2}$	h	36.3 ± 3.1	34.1 ± 1.4
MRT	h	44.9 ± 5.6	41.8 ± 2.1
C_{max}	ng mL^{-1}	418.5 ± 23.7	112.4 ± 8.4
T_{max}	h	4	2
$AUC_{0-\tau}$	ng mL^{-1} h	3821.4 ± 267.4	1529.0 ± 105.6
$AUC_{0-\infty}$	ng mL^{-1} h	4374.2 ± 344.1	2611.3 ± 153.6

Data are shown as mean ± SD
MRT mean residence time, *AUC* area under curve

Bioavailability

In vivo pharmacokinetic study for free silybin and silybin-loaded calcium phosphate microparticles was conducted in beagle dogs. Plasma concentration *versus* time profiles of silybin following oral administration of silybin-loaded calcium phosphate microparticles and free silybin are depicted in Fig. 5. The pharmacokinetic parameters simulated by non-compartmental model using software program BAPP 2.3 are also shown in Table I. As illustrated in the profile, the average value of C_{max} after oral administration of silybin-loaded calcium phosphate microparticles was 418.5±23.7 ng mL^{-1} with T_{max} of about 4 h as compared with C_{max} of 112.4± 8.4 ng mL^{-1} and T_{max} of about 2 h from the free silybin. In addition, the relative bioavailability of silybin-loaded calcium phosphate microparticles in contrast with free silybin was about 167.5%.

In Vitro–In Vivo Correlation

In this study, the correlation between *in vitro* and *in vivo* data for the prepared calcium phosphate microparticles was investigated. A level A correlation (32), *i.e.*, a point-to-point relationship between *in vitro* dissolution and *in vivo* absorption, was established in HCl solution (pH 1.2) and phosphate buffer solution (pH 7.4). As can be seen from Fig. 6, an excellent correlation was obtained with r=0.98917 for the phosphate buffer solution and r=0.98737 for HCl solution.

DISCUSSION

Povidone-mixed micelle system was initially designed to improve the solubility and oral bioavailability of poorly soluble drugs. PVP is a water-soluble nonionic polymer, which has a long history of use in pharmaceutical applications as a delivery system for poorly soluble drugs (33). Addition of PVP has been shown to increase the solubility and dissolution rates of certain poorly soluble drugs (34). In this study, the povidone-mixed micelle system was adopted innovatively as a new type of template to fabricate the calcium phosphate micron-sized carrier, which was incorporated with the hydrophobic drug, silybin, to evaluate oral bioavailability. As shown in Fig. 6, SEM images demonstrated the calcium phosphate carrier was well dispersed as individual particles. The particle size (3.5 μm) observed from the SEM was consistent with that determined by the particle detector. Furthermore, the calcium phosphate micron-sized carrier exhibited spherical or ellipsoidal shape with a rough surface, which suggested an irregular porous structure, thus proving that the micelle template was removed by solvent evaporation over a gentle temperature condition of 40°C. As shown in Fig. 6, the FTIR spectra confirmed the existence of calcium phosphate. The disappearance and decrease in spectra of drug-loaded calcium phosphate carrier at certain group bands of silybin indicated the incorporation of silybin into the porous structure.

As pointed out in our previous study, the dissolution of free silybin was pH-dependent which increased with increasing pH (15,16). In the present work, the drug release behavior of calcium phosphate carrier was conducted in different pH solution. It can be seen from Fig. 6 that the dissolution profile exhibited a faster release from the calcium phosphate carrier

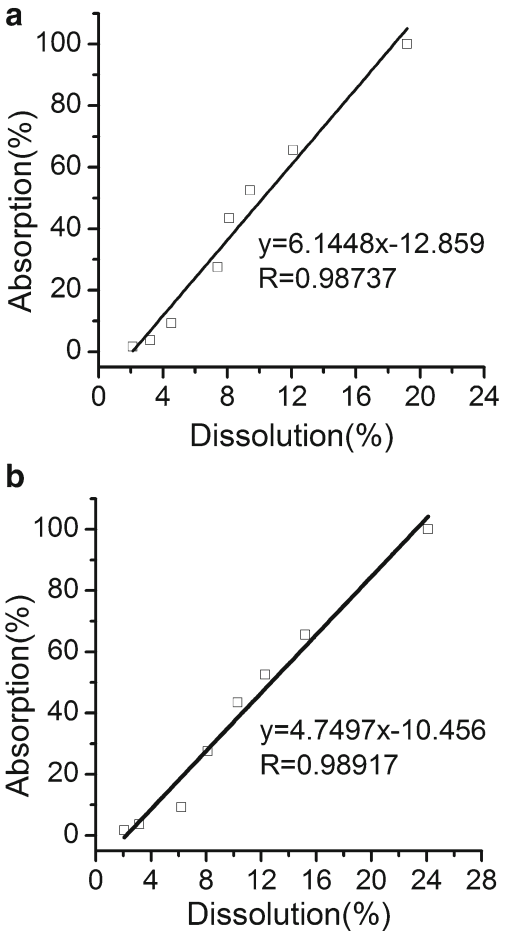

Fig. 6. Correlations between *in vitro* dissolution fractions and *in vivo* absorption fractions in two dissolution media. **a** pH 1.2 HCl solution. **b** pH 7.4 phosphate buffer solution

than free silybin, while the both release accelerated with increasing pH. The release behavior of silybin from the calcium phosphate microparticles was consistent with our previous findings. Therefore, the pH-dependent behavior might indicate the removal of templated micelles. The pH-dependent behavior of silybin-loaded calcium phosphate microparticles could mainly be attributed to the silybin itself. The dissolution rate from calcium phosphate carriers was markedly different due to the different templates involved, some exhibited a very fast release behavior (35) while others exhibited a slow release behavior (3).

The pharmacokinetics of silybin-loaded calcium phosphate carrier and free silybin after orally administrated to beagle dogs were also investigated in this work. As observed from the profile of plasma concentration *versus* time depicted in Fig. 6 and the pharmacokinetic parameters shown in Table I, free silybin exhibited a very low bioavailability, which was in conformity with the results previously reported (36,37). Meanwhile, the clinical efficacy of silybin is discounted by its poor water solubility, which result in poor oral absorption and bioavailability. Additionally, obvious differences between free silybin and silybin-loaded calcium phosphate carrier were found with respect to the delayed T_{max} from 2 to 4 h. Moreover, the peak concentration of silybin release was approximately 3.7-fold of the free silybin after it had been

incorporated into the calcium phosphate carrier. The main reason for the delay in T_{max} may be ascribed to the materials which we used for preparing the calcium phosphate microparticles. After the drug was incorporated into this carrier, it was protected by the microparticle matrix from the rapid degradation at acidic pH conditions. Notably, a tiny peak was observed at 10 h, which may be due to the effect of bile salt *via* the enterohepatic circulation, as evidenced by Wu *et al.* (38). The relative bioavailability of 167.5% for silybin-loaded calcium phosphate carrier was dramatically enhanced compared to the free silybin. However, no significant difference was found in $t_{1/2}$ and MRT between the two experimental groups. As we know, the micellar system has been extensively investigated due to its advantage in improving the solubility and enhancing the oral bioavailability of poorly water-soluble drug. In our experiment, the calcium phosphate microparticle designed from povidone/sodium cholate/phospholipid mixed micelles was successfully prepared, and the drug was proven to be incorporated into the porous structure after the removal of the micellar template, thus leading to prolonged release *in vitro* and enhanced absorption *in vivo*. On the other hand, the improved oral bioavailability of silybin-loaded microparticle might be attributed to enhanced silybin solubility in the gastrointestinal tract and relatively small size (39). Additionally, the drug was expected to be highly dispersed with high drug loading content in the prepared microparticle system due to the porous structure of the calcium phosphate microparticle.

The *in vitro–in vivo* correlation analysis of silybin-loaded calcium carbonate nanoparticles in two different media (phosphate buffer solution (pH 7.4) and HCl solution (pH 1.2)) showed an excellent linear relationship, with no significant influences of different pH values. This excellent correlation is quite important since it could suggest the possibility to predict *in vivo* pharmacokinetic behavior through the observed *in vitro* release profiles (40).

CONCLUSION

In summary, a novel porous calcium phosphate microparticle based on povidone/sodium cholate/phospholipid mixed micelles was prepared successfully for the first time. The pharmacokinetic study in beagle dogs showed the enhanced oral bioavailability facilitated by the prepared microparticle. The findings support the ability of porous calcium phosphate microparticle to improve solubility and oral bioavailability, thus advancing the literature of drug delivery for poorly water-soluble drugs.

ACKNOWLEDGMENTS

This work was supported by the National Natural Science Foundation of China (30472098), China Postdoctoral Science Foundation funded project (2015M571700), College Natural Science Research Foundation of Jiangsu Province (14KJB350002), and Research Foundation for Distinguished Scholars (15JDG074). This work was also funded by the Priority Academic Program Development of Jiangsu Higher Education Institutions. The authors are grateful to Emmanuel Omari-Siawat of Jiangsu University for correcting the English grammar. The authors also thank the University Ethics Committee for the kind guidance in the animal experiments.

COMPLIANCE WITH ETHICAL STANDARDS

Conflict of Interest The authors declare that they have no competing interests.

REFERENCES

1. Bohner M, Galea L, Doebelin N. Calcium phosphate bone graft substitutes: failures and hopes. J Eur Ceram Soc. 2012;32(11):2663–71.
2. Nouri A, Castro R, Santos JL, Fernandes C, Rodrigues JHT. Calcium phosphate-mediated gene delivery using simulated body fluid (SBF). Int J Pharm. 2012;434(434):199–208.
3. QL T, YJ Z, J W, F C, SW C. Calcium phosphate drug nanocarriers with ultrahigh and adjustable drug-loading capacity: one-step synthesis, in situ drug loading and prolonged drug release. Nanomedicine: nanotechnology, Biology,\s&\smedicine. 2011;7(4):428–434.
4. Azevedo HS, Leonor IB, Alves CM, Reis RL. Incorporation of proteins and enzymes at different stages of the preparation of calcium phosphate coatings on a degradable substrate by a biomimetic methodology. Mater Sci Eng C. 2005;25(2):169–79.
5. Majid K, Tseng MD, Baker KC, Reyes-Trocchia A, Herkowitz HN. Biomimetic calcium phosphate coatings as bone morphogenetic protein delivery systems in spinal fusion. Spine J. 2011;11(6):560–7.
6. Li J, Chen YC, Tseng YC, Mozumdar S, Huang L. Biodegradable calcium phosphate nanoparticle with lipid coating for systemic siRNA delivery. J Control Release. 2010;142(3):416–21.
7. Pittella F, Miyata K, Maeda Y, Suma T, Watanabe S, Chen Q, *et al.* Pancreatic cancer therapy by systemic administration of VEGF siRNA contained in calcium phosphate/charge-conversional polymer hybrid nanoparticles. J Control Release. 2012;161(3):868–74.
8. Asim N, Radiman S, Yarmo MA, Golriz MSB. Vanadium pentoxide: synthesis and characterization of nanorod and nanoparticle V2O5 using CTAB micelle solution. Microporous Mesoporous Mater. 2009;120(120):397–401.
9. Dasgupta S, Bandyopadhyay ASB. Reverse micelle-mediated synthesis of calcium phosphate nanocarriers for controlled release of bovine serum albumin. Acta Biomater. 2009;5(8):3112–21.
10. Chen BH, Chen KI, Ho ML, Chen HN, Chen WC, Wang CK. Synthesis of calcium phosphates and porous hydroxyapatite beads prepared by emulsion method. Mater Chem Phys. 2009;113(1):365–71.
11. Lai C, Tang SQ, Wang YJ, Wei K. Formation of calcium phosphate nanoparticles in reverse microemulsions. Mater Lett. 2005;59(2):210–4.
12. Fujiwara M, Shiokawa K, Morigaki K, Tatsu Y, Nakahara Y. Calcium phosphate composite materials including inorganic powders, BSA or duplex DNA prepared by W/O/W interfacial reaction method. Mater Sci Eng C. 2008;28:280–8.
13. Schmidt SM, McDonald J, Pineda ET, Verwilst AM, Chen Y, Josephs R, *et al.* Surfactant based assembly of mesoporous patterned calcium phosphate micron-sized rods. Microporous Mesoporous Mater. 2006;94:330–8.
14. Zhang J, Jiang D, Chen Z, Huang Z. Synthesis of calcium phosphate fluoride hybrid hollow spheres. Mater Lett. 2013;91(3):35–8.
15. Jiang-nan YU, Yuan ZHU, Li WANG, *et al.* Enhancement of oral bioavailability of the poorly water-soluble drug silybin by sodium cholate/ phospholipid-mixed micelles. Acta Pharmacol Sin. 2010;31(6):759–64.
16. Yuan Z, Yu J, Tong S, Li W, Min P, Xia C, *et al.* Preparation and in vitro evaluation of povidone-sodium cholate-phospholipid mixed micelles for the solubilization of poorly soluble drugs. Arch Pharm Res. 2010;33(6):911–7.
17. Sun N, Wei X, Wu B, Jian C, Yi L, Wei W. Enhanced dissolution of silymarin/polyvinylpyrrolidone solid dispersion pellets prepared by a one-step fluid-bed coating technique. Powder Technol. 2008;182(1):72–80.

18. Dongowski G, Fritzsch B, Giessler J, Hartl A, Kuhlmann O, Neubert RH. The influence of bile salts and mixed micelles on the pharmacokinetics of quinine in rabbits. Eur J Pharm Biopharm. 2005;60(1):147–51.
19. Hammad MA, Müller BW. Increasing drug solubility by means of bile salt–phosphatidylcholine-based mixed micelles. Eur J Pharm Biopharm Off J Arbeitsgemeinschaft Für Pharm Verfahrenstechnik E V. 1998;46(3):361–7.
20. Peter B, Pioletti DP, Laïb S, Bujoli B, Pilet P, Janvier P, *et al*. Calcium phosphate drug delivery system: influence of local zoledronate release on bone implant osteointegration. Bone. 2005;36(1):52–60.
21. Tang QL, Zhu YJ, Wu J, Chen F, Cao SW. Calcium phosphate drug nanocarriers with ultrahigh and adjustable drug loading capacity: one-step synthesis, in-situ drug loading and prolonged drug release. Nanomedicine Nanotechnol Biol Med. 2011;7(4):428–34.
22. Agarwal R, Katiyar SK, Lundgren DW, Mukhtar H. Inhibitory effect of silymarin, an anti-hepatotoxic flavonoid, on 12-O-tetradecanoylphorbol-13-acetate-induced epidermal ornithine decarboxylase activity and mRNA in SENCAR mice. Carcinogenesis. 1994;15:20.
23. Flora K, Hahn M, Rosen H, Benner K. Milk thistle (Silybum marianum) for the therapy of liver disease. Am J Gastroenterol. 1998;93(2):139–43. **21**.
24. Loguercio C, Andreone P, Brisc C, Brisc MC, Bugianesi E, Chiaramonte M, *et al*. Silybin combined with phosphatidylcholine and vitamin E in patients with nonalcoholic fatty liver disease: a randomized controlled trial. Free Radic Biol Med. 2012;52(9):1658–65. **22**.
25. Tedesco D. Effects of silymarin, a natural hepatoprotector, in periparturient dairy cows. J Dairy Sci. 2004;87(7):2239–2247. 23.
26. Ligeret H, Brault A, Vallerand D, Haddad Y, Haddad PS. Antioxidant and mitochondrial protective effects of silibinin in cold preservation-warm reperfusion liver injury. J Ethnopharmacol. 2008;115(3):507–14. **24**.
27. Abenavoli L, Capasso R, Milic NFC. Milk thistle in liver diseases: past, present, future. Phytother Res Ptr. 2010;24(10):1423–32. **25**.
28. Zhu Y, Zhang J, Fu M, Zeng J, Omari-Siaw E, Xu XM. Calcium carbonate nanoparticles templated by mixed polymeric micelles: characterization, in vitro drug release and oral bioavailability in beagle dogs. Latin American Journal of Pharmacy. 2014;33. 26.
29. Chen L, Zhu H, Yang S, Zhou B, You F, Yan X. Nanostructured calcium phosphate carriers for deliver of poor water-soluble drug silybin. Materials Letters. 2015:252–255. 27.
30. Usman M, Ahmad M, Dayo A, Madni A, Ali L, Yousuf M, *et al*. Effect of &BETA;-Glucuronidase on extraction efficiency of silymarin from human plasma samples using validated HPLC-UV analysis. Trop J Pharm Res. 2012;11(1):84–90.
31. Bssman J, Reppas C. In vitro–in vivo correlations for lipophilic, poorly water-soluble drugs. Eur J Pharm Sci. 2000;11:S73–80. **29**.
32. Zhu Y, Peng W, Zhang J, Wang M, Firempong CK, Feng C, *et al*. Enhanced oral bioavailability of capsaicin in mixed polymeric micelles: preparation, in vitro and in vivo evaluation. J Funct Foods. 2014;8(3):358–66. **30**.
33. Modi A, Tayade P. Enhancement of dissolution profile by solid dispersion (kneading) technique. Aaps Pharmscitech. 2006;7(3):E87–92.
34. Ahire BR, Rane BR, Bakliwal SR, Pawar SP. Solubility enhancement of poorly water soluble drug by solid dispersion techniques. Int J Pharmtech Res. 2010;3:2007–15.
35. Feng Y, Guo H, Zhang H, He X. Polymeric micelle-templated synthesis of hydroxyapatite hollow nanoparticles for a drug delivery system. Acta Biomater. 2010;6(6):2212–8.
36. Morazzoni P, Magistretti MJ, Giachetti C, Zanolo G. Comparative bioavailability of Silipide, a new flavanolignan complex, in rats. Eur J Drug Metab Pharmacokinet. 1992;17(1):39–44.
37. Wei Y, Ye X, Shang X, Peng X, Bao Q. Enhanced oral bioavailability of silybin by a supersaturatable self-emulsifying drug delivery system (S-SEDDS). Colloids Surf A Physicochem Eng Asp. 2012;396(7):22–8.
38. Wu W, Wang Y, Que L. Enhanced bioavailability of silymarin by self-microemulsifying drug delivery system. Eur J Pharm Biopharm. 2006;63(3):288–94.
39. Dou J, Zhang H, Liu X, Zhang M, Zhai G. Preparation and evaluation in vitro and in vivo of docetaxel loaded mixed micelles for oral administration. Colloids Surf B: Biointerfaces. 2014;114(2):20–7.
40. Borkar N, Xia D, Holm R, Gan Y, Müllertz A, Yang M, *et al*. Investigating the correlation between in vivo absorption and in vitro release of fenofibrate from lipid matrix particles in biorelevant medium. Eur J Pharm Sci. 2013;51(1):204–10.